Influence of ground control points and processing parameters on UAS image mosaicking for plant height estimation

Chenghai Yang[1], Hengqian Zhao[2], Wei Guo[3], Jian Zhang[4]
Charles Suh[1], Bradley Fritz[1]

[1]USDA-ARS, College Station, Texas, USA
[2]China University of Mining and Technology, Beijing, China
[3]Henan Agricultural University, Zhengzhou, Henan, China
[4]Huazhong Agricultural University, Wuhan, Hubei, China
[2,3,4]Former Visiting Scholars

A paper from the Proceedings of the
16th International Conference on Precision Agriculture
21-24 July 2024
Manhattan, Kansas, United States

Abstract.

Three-dimensional (3D) point clouds and digital surface models (DSMs), generated using overlapping images from unmanned aircraft systems (UASs), are often used for plant height estimation in phenotyping and precision agriculture. This study examined the effects of the quantity and placement of ground control points (GCPs) and image processing parameters on the creation of 3D point clouds and DSMs for plant height estimation. A 2-ha field containing multiple experimental plots with four crops (corn, cotton, sorghum, and soybean) was used for this study. Thirty-six panels were systematically positioned across these plots, with 12 at ground level and 12 each at approximately 0.75 m and 1.5 m above ground. Aerial images were captured at 60 m above ground level using a rotary hexacopter equipped with a Nikon D7100 camera. Plant height was manually measured from 48 sampling points among the four crops. Orthomosaics, 3D point clouds, and DSMs with various GCP configurations and processing parameter combinations were generated using Pix4Dmapper software. Results showed that increasing GCPs from one to five reduced the total positional root mean square error (RMSE) from 2.3 m to 3 cm. However, adding more GCPs only marginally reduced RMSE to approximately 2-3 cm. Panel positions on or above the ground did not notably affect positional accuracy. Statistical analysis showed that the correlation coefficients between ground-measured and point cloud-extracted values were similar and consistent with four or more GCPs. Moreover,

point cloud-based plant height estimates were more accurate and consistent than DSM-based estimates. Changing image processing settings, including keypoint image scale, densification image scale, point density, and minimum number of point-to-image matches, directly affected the number of 3D points created, processing time, and plant height estimation. The results from this study provide practical guidance for selecting suitable GCPs and image processing parameters for accurate plant height estimation with UAS imagery in test plots and small fields.
Keywords.
Aerial image, digital surface model, plant height, point cloud, unmanned aircraft system.

Introduction

Unmanned aircraft systems (UAS) have become indispensable remote sensing tools for precision agriculture. By capturing overlapping high-resolution imagery, UAS enable the creation of orthomosaic images as well as 3D point clouds and digital surface models (DSMs), providing valuable information about the structure of crops (Bendig et al., 2014; Corti et al., 2023). These datasets facilitate accurate measurement of plant height, biomass, and yield potential (Chang et al., 2017; Gilliot et al., 2021). Furthermore, 3D modeling of crop plants allows for the characterization of plant geometry, enabling researchers and agronomists to analyze canopy structure, describe leaf features, and distinguish weeds from crops (Harandi et al., 2023). The photogrammetric method used for 3D reconstruction from a series of overlapping, offset images captured by a moving sensor is known as structure-from-motion (SfM). The accuracy of 3D point clouds and associated products is influenced by various factors such as camera types, flight parameters, the number and distribution of ground control points (GCPs), and processing methods and parameter settings (Westoby et al., 2012; Liu et al., 2022; Du et al., 2024). The effects of the number and distribution of GCPs on the positional accuracy of orthomosaics have been studied (Rangel et al., 2018; Sanz-Ablanedo et al., 2018; Oniga et al., 2020) across different land types.

Achieving high positional accuracy in 3D point cloud modeling necessitates the strategic placement of an adequate number of GCPs. Ideally, these points should be evenly distributed across both the periphery and center of the imaging area (Harvin et al., 2015; Martínez-Carricondo et al., 2018; Ulvi, 2021). The optimal number and spatial arrangement of GCPs vary depending on factors such as the size and topography of the study area. Generally, larger areas require more GCPs for accurate reconstruction (Sanz-Ablanedo et al., 2018). Multiple studies have suggested varying numbers of GCPs and their spatial distributions based on the imaging size and number of images (Agüera-Vega et al., 2017; Rangel et al., 2018; Oniga et al., 2020). While placing GCPs in the field and adding them to a project during image processing can be time-consuming, it is more efficient than having to redo a project due to insufficient accuracy.

SfM methods have been extensively utilized in phenotyping and precision agriculture applications to estimate crop height from UAS images (Holman et al., 2016; Malambo et al., 2018; Xie et al., 2021). These studies have demonstrated significant correlations between UAS-based estimates and ground or LiDAR data. However, few have investigated the impact of GCPs on positional accuracy and plant height estimation in small-plot experimental and crop fields. Most studies examining the effect of GCPs on positional accuracy and 3D modeling have focused on non-crop areas. Another important factor influencing the accuracy of 3D point cloud construction is the selection of the processing parameters within SfM-based software. While default settings often yield satisfactory results for various applications, fine-tuning these processing settings can enhance both the accuracy and efficiency of 3D construction (James et al., 2017). Since Pix4Dmapper Pro is widely used for research and commercial applications, it is necessary to explore the effects of processing parameter selection on the accuracy and efficiency of creating 3D point clouds and DSMs for plant height estimation.

Therefore, the objectives of this study were to: 1) examine the effects of GCP quantity and placement on the positional accuracy of 3D point clouds and the accuracy of plant height estimation; and 2) evaluate how various processing parameters in Pix4Dmapper Pro affect the

generation and processing time of 3D point clouds and DSMs.

Materials and methods

Layout of crop plots and ground control panels

This study was conducted over a 2-ha area (30°31'19.2"N, 96°24'0.7"W) at the Texas A&M University AgriLife Research Farm near College Station, Texas, USA. Four crops, including cotton, corn, grain sorghum and soybeans, were planted in the northwest portion of the field in 16 plots with four replications (Fig. 1). Cotton with different nitrogen treatments was planted in the southeast portion of the field. To examine the effects of GCP quantity and placement on the positional accuracy of mosaicked imagery, a total of 36 white ground control panels with dimensions of 0.3 m by 0.3 m were systematically positioned across these plots, with 12 at ground level, 12 at 0.75 m above ground level (AGL), and 12 at 1.5 m AGL (Fig. 1). The center coordinates (x, y, z) of the panels were measured using a centimeter-grade R2 GNSS receiver with the virtual reference station (VRS) real-time kinematic (RTK) corrections (Trimble Inc., Westminster, Colorado, USA).

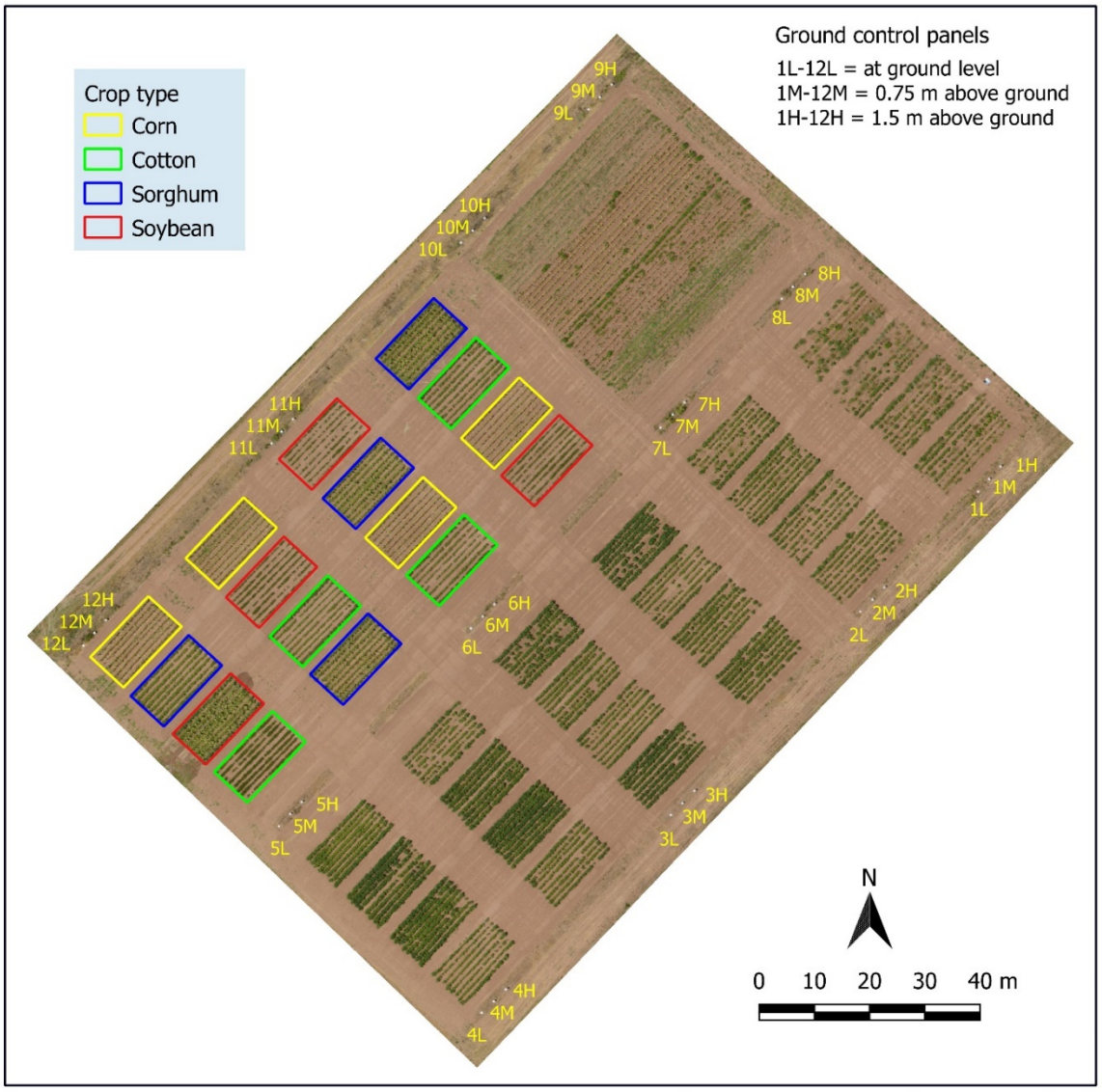

Fig. 1. Layout for crop plots and ground control panels across a 2-ha experimental field near College Station, TX. Plant height data collected from the 16 color-coded plots in the northwest portion of the field were used in this study. Each plot measured approximately 8 m by 15 m.

UAS image acquisition

A rotary AG-V6A hexacopter UAS (Homeland Surveillance & Electronics, LLC, Casselberry, Florida, USA), equipped with a consumer-grade Nikon D7100 camera (Nikon Inc., Melville, NY), was used for image acquisition. RGB images with a pixel array of 6000 x 4000 were captured for this study. Image acquisition was conducted along 13 flight lines at an altitude of 60 m AGL with a similar side and front overlap of 83%. The resulting pixel size was approximately 1.0 cm. Plant height was manually measured at three selected plant canopies in each of the 16 plots. The geographic coordinates for the 48 sampling locations were measured with the Trimble R2 GNSS receiver.

Configurations of GCPs for positional accuracy assessment

For the evaluation of GCP quantity and placement on positional accuracy, various numbers of GCPs were arranged in 29 different configurations across the study area (Table 1). Configuration LMH0 had no GCP. Configurations L1-L6 consisted of 1-6 GCPs at ground level, while configurations L9 and L12 contained 9 and 12 GCPs, respectively, at ground level. The same pattern was repeated for the GCPs at the other two ground levels. Configurations LM24, LH24 and MH24 each consisted of 24 GCPs for the combinations of any two panel levels, and configuration LMH36 had all 36 GCPs.

Table 1. Configurations of ground control points (GCPs) for positional accuracy assessment

Configuration	Number of GCPs	Distribution of GCPs
LMH0	0	None
L1	1	6L
L2	2	5L,8L
L3	3	1L,4L,9L
L4	4	1L,4L,9L,12L
L5	5	1L,4L,9L,12L,6L
L6	6	1L,4L,9L,12L,6L,7L
L9	9	1L,4L,9L,12L,6L,7L,3L,5L,11L
L12	12	1L-12L
M1	1	6M
M2	2	5M,8M
M3	3	1M,4M,9M
M4	4	1M,4M,9M,12M
M5	5	1M,4M,9M,12M,6M
M6	6	1M,4M,9M,12M,6M,7M
M9	9	1M,4M,9M,12M,6M,7M,3M,5M,11M
M12	12	1M-12M
H1	1	6H
H2	2	5H,8H
H3	3	1H,4H,9H
H4	4	1H,4H,9H,12H
H5	5	1H,4H,9H,12H,6H
H6	6	1H,4H,9H,12H,6H,7H
H9	9	1H,4H,9H,12H,6H,7H,3H,5H,11H
H12	12	1H-12H
LM24	24	1L-12L,1M-12M
LH24	24	1L-12L,1H-12H
MH24	24	1M-12M,1H-12H
LMH36	36	1L-12L,1M-12M,1H-12H

Image processing for determining the effect of GCP configurations

Pix4Dmapper Pro (Pix4D S.A., Prilly, Switzerland) installed on a Dell Precision 7920 workstation with a RAM of 128 GB and a dual processor motherboard was used for image processing in this study. Image processing in Pix4Dmapper Pro involves three general steps: 1) Initial processing, 2) Point cloud and mesh, and 3) DSM, orthomosaic and index. After the initial processing step, all 36 GCPs were added to the initial project. Each control point was marked on all RGB images that contained the ground control panel.

For each GCP configuration, a different number of GCPs were used as control points as shown in Table 1, and the rest of the GCPs were used as check points for accuracy assessment. For

example, configuration LMH0 used no GCP as control points with all 36 GCPs as check points. Conversely, configuration LMH36 used all 36 GCPs as control points with no GCP as check points. The rest of the configurations had varying numbers GCPs as control and check points. A total of 29 projects, one for each GCP configuration, were generated from the initial project for evaluation in this study.

The project for each GCP configuration was reprocessed for the first step again to take into account of the GCPs, and a quality report was created for the project. The positional errors of GCPs were included in the report for both control points and check points. Ideally, the errors for control points should be minimal, as they serve as the basis for aligning the entire dataset. Check points, on the other hand, were not used during the initial processing but were instead used to assess the accuracy of the generated 3D models and maps. For both control and check points, the following errors are calculated in Pix4DMapper:

$$Mean = \frac{1}{N} \sum_{i=1}^{N} e_i \quad (1)$$

$$STD = \sqrt{\frac{1}{N} \sum_{i=1}^{N} (e_i - Mean)^2} \quad (2)$$

$$RMSE = \sqrt{\frac{1}{N} \sum_{i=1}^{N} {e_i}^2} \quad (3)$$

where e_i is the error between calculated position and measured position of point i for the given direction (X,Y,Z), and *N* is the number of control or check points. Mean is the average error in each direction, STD is the standard deviation of the error in each direction, and RMSE is the root mean square error in each direction. To evaluate the total error in all three directions, the total RMSE was calculated using the following formula:

$$RMSE_{total} = \sqrt{RMSE_x^2 + RMSE_y^2 + RMSE_z^2} \quad (4)$$

Creation of point clouds and DSM using various processing parameters

For each of the three steps in Pix4Dmapper Pro, various options are available to allow the user to define appropriate processing parameters. For step 1, the extraction of keypoints from the images is essential. Keypoints are points or pixels with easily recognizable contrast and texture and they can be extracted using five keypoint image scales: 1, 2, 1/2, 1/4, and 1/8. A scale of 1 represents the original image size (default), while a scale of 2 doubles the image size in both directions. The other three scales can be used to speed up processing by using only portions of the full image size. A larger image scale tends to extract more keypoints with longer processing time. Step 2 involves point cloud densification, and three parameters can be selected, including image scale, point density, and minimum number of matches.

As in step 1, the image scale defines the scale at which additional 3D points are computed, and four options are available for selection: 1, 1/2 (default), 1/4, and 1/8. Point density defines the density of the densified point cloud and it has the options of High (slow), Optimal (default), and Low (fast). The minimum number of matches represents the minimum number of valid reprojections of each 3D point to the images. The minimum number of matches can vary from 2 to 6 with 3 being the default. More matches reduce the noise and improve the quality of point cloud, but it may compute fewer 3D points in the final point cloud. For step 3, the options are used to select the spatial resolution to generate DSM and orthomosaic images, DSM filters to filter and smooth points of the point cloud, and methods (inverse distance weighing or triangulation) to generate the DSM raster.

To evaluate the effects of these parameters on processing results, the RGB images and all 36 GCPs were used. With all the options, hundreds of possible combinations can be selected for processing each set of images. There are a total of 300 (5x4x3x5) possible combinations or projects for steps 1 and 2. In this study, only 14 selected representative combinations were processed to evaluate the effects of these options, as each combination took a few hours to run.

Specifically, the images were processed using all five keypoint image scales in step 1 with the default setting in step 2, resulting in five projects. Then the images were processed by changing the following parameters in step 2 one at a time with all other settings set to defaults: three densification image scales (1, 1/4, 1/8), two levels of point density (Low and High), and four minimum numbers of matches (2, 4, 5, 6). For step 3, all default settings were used except that triangulation was selected as the DSM generation method. To evaluate the effects of GCP quantity and distribution on processing results, the RGB images with 11 GCP configurations (L4, L5, L6, L9, L12, M12, H12, LM24, LH24, MH24, and LMH36) were processed using default settings in steps 1 and 2.

Extraction of plant height from point clouds and DSMs

To estimate plant height, circles with a diameter of 30 cm centered at each of the 48 sampling points were used to extract all the points falling within the circles in the point clouds and DSMs. The ground elevation values measured by the GPS at the sampling sites were then subtracted from the extracted elevation points as estimated plant height data. The 90^{th}, 95^{th}, 99^{th}, and 100^{th} percentiles of the estimated height data were calculated for the 48 samples.

Correlation and regression ananlyses

Correlation analysis was performed to determine the correlations between measured plant height and the percentiles derived from the DSMs and point clouds for the 11 GCP configurations and the 14 combinations of processing parameters. The correlation results were used to examine the effects of processing parameters and GCP configurations on plant height estimation. Linear regression was performed between measured plant height and the best percentiles for plant height estimation. Python programs were written to automatically extract plant height estimates from the point clouds and DSMs and to perform correlation analysis between measured and estimated plant height data.

Results and discussion

Directional and total RMSE

Table 2 shows the RMSE in each direction (X,Y,Z) and the total RMSE for both control points and check points for each of the 29 GCP configurations based on the RGB images. The RMSE for control points generally increased with the number of control points. When no GCP was used, the RMSE values for the check points were 0.559 m, 0.594 m, and 6.575 m, respectively, in the X, Y, and Z directions with a total RMSE of 6.625 m. The vertical error was much higher than the horizontal errors. As more GCPs at ground level were used as control points, the directional and total RMSE values for the check points generally decreased and stabilized with four or more GCPs. This trend was true for the panels placed at the other two higher ground levels. Although the RMSE values were slightly different among the three GCP levels, they were practically the same, indicating that panel positions on or above the ground did not notably affect positional accuracy. This observation was further confirmed by the similar RMSE values for the three configurations (LM24, LH24, MH24) involving the combinations of any two panel levels.

Effects of GCP configuration on plant height estimation

Table 3 summarizes the correlation coefficients between ground-measured plant height and estimated values based on the point clouds and DSMs for the 11 different GCP configurations. Correlation coefficients for the point cloud-based estimates had most of the highest values at the 99^{th} percentile, while those for the DSM-based estimates had most of the highest values at the 100^{th} percentile or the maximum. The correlations based on the point clouds (ranging from 0.964 to 0.976) were generally higher than those based on the DSMs (ranging from 0.889-0.967). These results indicated that the point cloud-based method was more accurate and consistent than the DSM-based method for plant height extraction. Interestingly, the highest correlation values based

on the point clouds were very consistent among the 11 GCP configurations, indicating that 4-6 GCPs were sufficient for accurate plant height estimation. The vertical positions of the GCPs had little effect on the point cloud-based results.

Table 2. Root mean square error (RMSE) in XYZ and total RMSE for both control points and check points for 29 ground control point (GCP) configurations based on RGB images collected from a test field at 60 m.

GCP configuration	Control points and RMSE (m)					Check points and RMSE (m)				
	Quantity	X	Y	Z	Total	Quantity	X	Y	Z	Total
LMH0	0	-	-	-	-	36	0.559	0.594	6.575	6.625
L1	1	0.000	0.000	0.000	0.000	35	1.074	1.071	1.726	2.297
L2	2	0.001	0.000	0.001	0.001	34	0.082	0.095	1.109	1.116
L3	3	0.004	0.002	0.000	0.004	33	0.015	0.037	0.032	0.051
L4	4	0.009	0.010	0.005	0.014	32	0.010	0.020	0.020	0.030
L5	5	0.011	0.012	0.004	0.017	31	0.009	0.017	0.022	0.029
L6	6	0.009	0.009	0.004	0.013	30	0.010	0.018	0.021	0.029
L9	9	0.010	0.009	0.006	0.015	27	0.009	0.015	0.020	0.027
L12	12	0.010	0.009	0.008	0.016	24	0.010	0.015	0.020	0.027
M1	1	0.000	0.000	0.000	0.000	35	1.071	1.043	1.658	2.233
M2	2	0.001	0.000	0.001	0.001	34	0.079	0.089	1.115	1.121
M3	3	0.004	0.002	0.000	0.004	33	0.015	0.025	0.028	0.040
M4	4	0.006	0.006	0.001	0.009	32	0.012	0.015	0.028	0.034
M5	5	0.007	0.012	0.001	0.014	31	0.012	0.013	0.026	0.031
M6	6	0.008	0.011	0.001	0.014	30	0.013	0.013	0.026	0.032
M9	9	0.010	0.013	0.009	0.019	27	0.012	0.010	0.018	0.024
M12	12	0.010	0.013	0.008	0.018	24	0.012	0.011	0.017	0.023
H1	1	0.000	0.000	0.000	0.000	35	1.051	1.029	1.577	2.156
H2	2	0.001	0.000	0.001	0.001	34	0.082	0.062	1.134	1.138
H3	3	0.004	0.002	0.000	0.004	33	0.013	0.020	0.030	0.038
H4	4	0.006	0.006	0.001	0.009	32	0.013	0.012	0.022	0.028
H5	5	0.006	0.006	0.001	0.008	31	0.013	0.013	0.019	0.026
H6	6	0.007	0.006	0.002	0.010	30	0.012	0.013	0.019	0.027
H9	9	0.010	0.008	0.006	0.015	27	0.012	0.014	0.020	0.027
H12	12	0.010	0.008	0.008	0.016	24	0.012	0.014	0.020	0.027
LM24	24	0.010	0.011	0.011	0.019	12	0.010	0.012	0.018	0.024
LH24	24	0.010	0.010	0.012	0.019	12	0.010	0.014	0.017	0.024
MH24	24	0.010	0.011	0.012	0.019	12	0.012	0.011	0.018	0.024
LMH36	36	0.010	0.011	0.013	0.020	0	-	-	-	-

Table 3. Correlation coefficients (r) between measured plant height and estimated plant height from digital surface models (DSMs) and point clouds for different ground control point (GCP) configurations.

Data source	Percentile	GCP configuration										
		L4	L5	L6	L9	L12	M12	H12	LM24	LH24	MH24	LMH36
Point cloud	90th	0.891	0.950	0.936	0.929	0.945	0.887	0.917	0.936	0.933	0.929	0.956
	95th	0.931	0.965	0.965	0.964	0.974	0.923	0.958	0.952	0.963	0.957	0.971
	99th	**0.964**	**0.972**	**0.974**	**0.973**	**0.974**	0.959	**0.964**	**0.968**	0.974	**0.971**	**0.975**
	100th	0.960	0.953	**0.974**	0.969	0.973	**0.976**	0.958	0.965	**0.976**	**0.971**	**0.975**
DSM	90th	0.651	0.708	0.680	0.636	0.617	0.595	0.666	0.752	0.711	0.669	0.646
	95th	0.744	0.828	0.790	0.745	0.739	0.696	0.761	0.842	0.812	0.773	0.739
	99th	0.877	**0.927**	0.886	0.866	0.884	0.870	0.867	0.923	**0.926**	0.903	0.902
	100th	**0.908**	0.905	**0.930**	**0.891**	**0.914**	**0.967**	**0.915**	**0.945**	0.923	**0.945**	**0.940**

Bold r values indicate maximum values among the four percentiles for each GCP configuration.

Fig. 2 shows the scatterplots and regression lines between ground measured plant height and estimated values for GCP configurations L6 and LMH36 based on the point clouds and DSMs. The point cloud-based estimates provided a stronger linear relation than the DSM-based estimates. Plant height was less than 0.8 m for cotton and soybean but was much higher for sorghum and corn. It appears that the DSM-based estimates for the two taller crops were noisier than those for the other two crops. Cotton and soybean had relatively uniform and smooth canopies compared with the uneven and open canopies in sorghum and corn.

Effects of processing parameters in Pix4Dmapper Pro on plant height estimation

Table 4 summarizes the number of 3D points created and processing time as well as correlation coefficients between measured plant height and estimated values based on the point clouds for the 14 different combinations of processing parameters in Pix4Dmapper Pro. When keypoint image scale decreased from 2 to 1/8 with 1 being the default, the numbers of 3D points created

were essentially the same, approximately 50 million (M). However, processing time reduced from 2 hours 48 minutes for the scale of 2 to 1 hour 44 minutes for the scale of 1/8. Despite the large time differences, the correlation coefficients among the five keypoint image scales were generally consistent, ranging from 0.954 to 0.977 for the 99th percentile. Interestingly, the two smaller keypoint image scales had higher correlation values and shorter processing times than the other three scales.

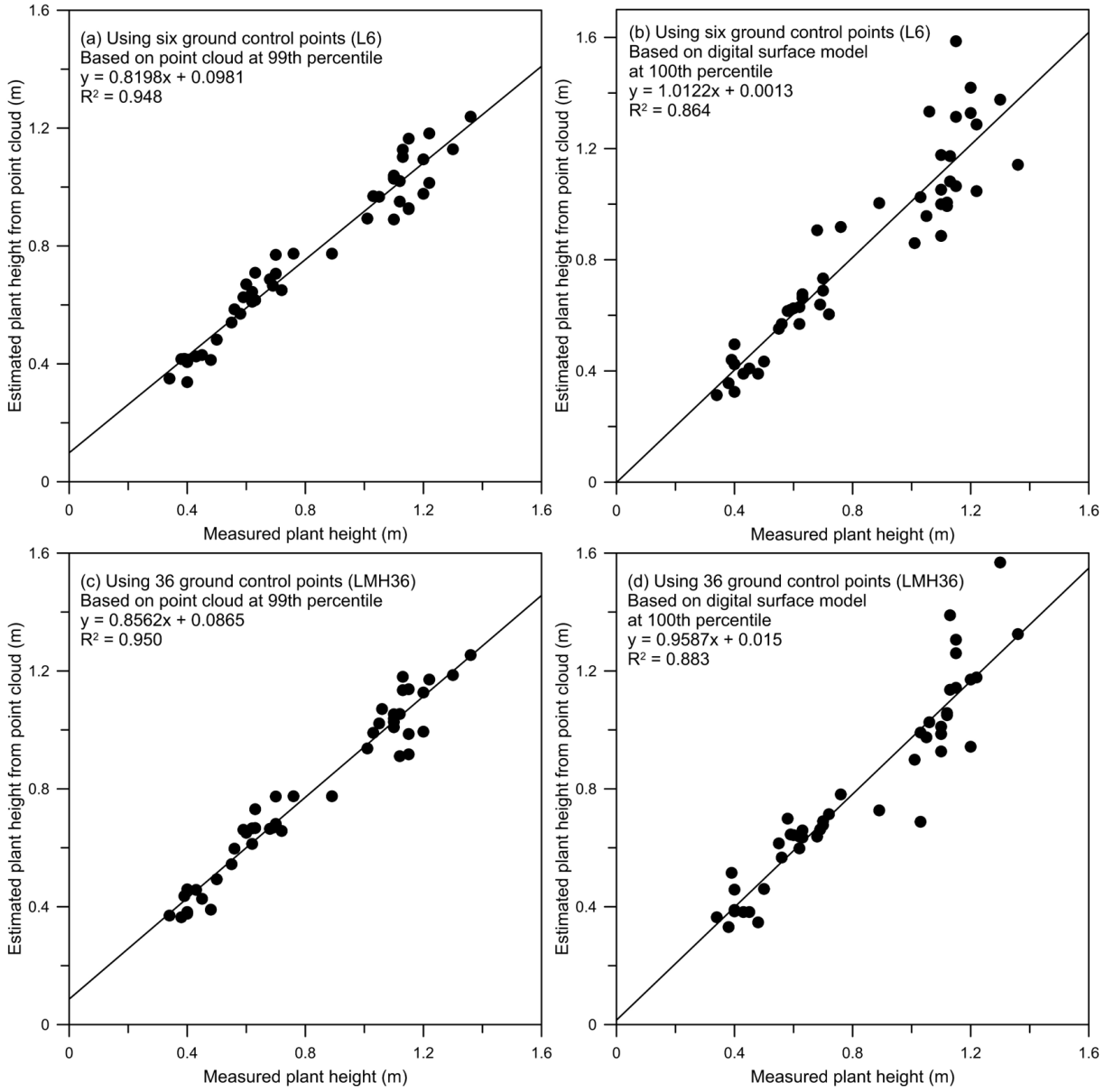

Fig. 2. Scatterplots and regression lines between measured plant height and estimated values based on (a) six ground control points (GCPs) and point cloud, (b) six GCPs and digital surface model (DSM), c) 36 GCPs and point cloud, and d) 36 GCPs and DSM.

By reducing densification image scale from 1 to 1/8 with 1/2 being the default listed in row 1, the number of 3D points was reduced from 177.7M to 2.9M and the respective processing time decreased from 5 hours 14 minutes to 1 hour 47 minutes. Meanwhile, the correlations for the 99th percentile decreased from 0.971 to 0.719. The much lower correlation value for the 1/8 scale indicated that this is not an appropriate choice. Although the scale of 1 had a higher r-value than the scale of 1/2 or 1/4, the longer processing time made it an inefficient choice. Changing point density from Low to High with the default being Optimal increased the number of 3D points from 14.0M to 175.7M and increased the processing time from 1 hour 56 minutes to 4 hours 13 minutes. The correlation coefficient for the 100th percentile increased from 0.931 to 0.980. The

High option has the potential for improved results if time permits. When the minimum number of matches changed from 2 to 6 with the default of 3, the number of 3D points created decreased from 67.2M to 30.9M, but the processing times were similar. However, the default minimum match number 3 had the best r-value, while the match number 6 had the lowest r-value, making it an inappropriate choice.

Fig. 3 shows the scatterplots and regression lines between ground measured plant height and estimated values based on the point clouds for the parameter combinations (1/4, 1/2, Optimal, 3) and (1, 1/2, High, 3). Although the combination (1, 1/2, High, 3) provided a slightly better r-squared value than the combination (1/4, 1/2, Optimal, 3), it took more than three times as long to process the project. From this preliminary analysis, a keypoint image scale of 1/4 or 1/8 in step 1 and the default settings in step 2 in Pix4Dmapper Pro appeared to be optimal parameter combinations.

Table 4. Number of 3D points created and processing time as well as correlation coefficients (r) between measured plant height and estimated values from point clouds for different processing parameters in Pix4Dmapper Pro.

Processing parameters				Number of 3D points created	Processing time	Plant height percentile			
Keypoint image scale	Densification image scale	Point density	Minimum number of matches			90th	95th	99th	100th
1	1/2	Optimal	3	49.9M	02h38m	0.936	0.955	0.962	**0.964**
2	1/2	Optimal	3	49.8M	02h48m	0.909	0.948	**0.967**	0.959
1/2	1/2	Optimal	3	50.0M	02h28m	0.870	0.932	**0.954**	0.953
1/4	1/2	Optimal	3	49.8M	02h03m	0.928	0.959	**0.975**	0.973
1/8	1/2	Optimal	3	50.2M	01h44m	0.919	0.967	**0.977**	0.969
1	1	Optimal	3	177.7M	05h14m	0.907	0.948	0.962	**0.971**
1	1/4	Optimal	3	11.7M	01h55m	0.845	0.898	0.950	**0.956**
1	1/8	Optimal	3	2.9M	01h47m	0.669	0.698	0.716	**0.719**
1	1/2	Low	3	14.0M	01h56m	0.844	0.897	**0.937**	0.931
1	1/2	High	3	175.7M	04h13m	0.914	0.954	0.971	**0.980**
1	1/2	Optimal	2	67.2M	02h40m	0.886	0.922	**0.949**	0.945
1	1/2	Optimal	4	41.0M	02h31m	0.924	0.948	**0.958**	0.956
1	1/2	Optimal	5	35.1M	02h25m	0.806	0.890	0.948	**0.949**
1	1/2	Optimal	6	30.9M	02h23m	0.602	0.658	0.694	**0.709**

Bold r values indicate maximum values among the four percentiles.

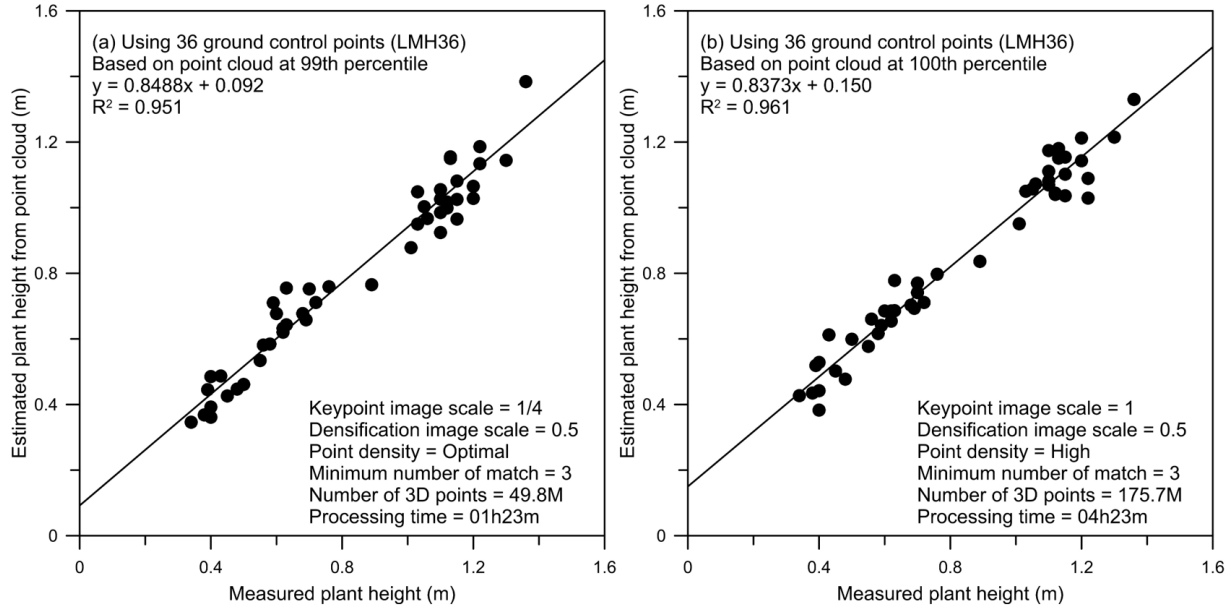

Fig. 3. Scatterplots and regression lines between measured plant height and estimated values based on two different combinations of processing parameters in Pix4Dmapper Pro shown in a) and b).

Summary

The results from this study demonstrate that GCP quantity and placement affect the positional

accuracy of the image products, but GCP positions on or above the ground do not notably affect positional accuracy. Although a minimum of four GCPs generally produce acceptable positional accuracy and height estimation, 6-9 GCPs on the ground may provide more accurate and consistent positional accuracy. It appears that the point cloud is superior to the DSM for plant height estimation. Additionally, the selection of processing parameters in Pix4Dmapper Pro directly affects the number and quality of the 3D points created in a point cloud as well as the processing time. Although the default settings provide balanced results, other appropriate combinations of parameters have the potential to improve accuracy and reduce processing time. More image data from other dates will be analyzed to further validate these preliminary findings.

Acknowledgements

The authors wish to thank Mike O'Neil for preparing and taking care of the test plots and Fred Gomez for assisting in field data collection. Mention of trade names or commercial products in this article is solely for the purpose of providing specific information and does not imply recommendation or endorsement by the U.S. Department of Agriculture. USDA is an equal opportunity provider and employer.

References

Agüera-Vega, F., Carvajal-Ramírez, F., & Martínez-Carricondo, P. (2017). Assessment of photogrammetric mapping accuracy based on variation ground control points number using unmanned aerial vehicle. *Measurement*, 98, 221-227. https://doi.org/10.1016/j.measurement.2016.12.002

Bendig, J., Bolten, A., Bennertz, S., Broscheit, J., Eichfuss, S., & Bareth, G. (2014). Estimating biomass of barley using Crop Surface Models (CSMs) derived from UAV-based RGB imaging. *Remote Sensing,* 6, 10395–10412.

Chang, A., Jung, J., Maeda, M. M., & Landivar, J. (2017). Crop height monitoring with digital imagery from Unmanned Aerial System (UAS). *Computers and Electronics in Agriculture*, 141, 232–237. https://doi.org/10.1016/j.compag.2017.07.008

Corti, M., Cavalli, D., Cabassi, G., Martina Corti, Daniele Cavalli, Giovanni Cabassi, Bechini, L., Pricca, N., Paolo, D., Marinoni, L., Vigoni, A., Degano, L., & Marino, P. (2023). Improved estimation of herbaceous crop aboveground biomass using UAV-derived crop height combined with vegetation indices. *Precision Agriculture,* 24, 587–606. https://doi.org/10.1007/s11119-022-09960-w

Du, X., Zheng, L., Zhu, J., Cen, H., & He, Y. (2024). Evaluation of mosaic image quality and analysis of influencing factors based on UAVs. *Drones,* 8, 143. https://doi.org/10.3390/drones8040143

Gilliot, J. M., Michelin, J., Hadjard, D., & Houotet, S. 2021. An accurate method for predicting spatial variability of maize yield from UAV-based plant height estimation: a tool for monitoring agronomic field experiments. *Precision Agriculture,* 22, 897–921. https://doi.org/10.1007/s11119-020-09764-w

Harwin, S., Lucieer, A., & Osborn, J. (2015). The impact of the calibration method on the accuracy of point clouds derived using unmanned aerial vehicle multi-view stereopsis. *Remote Sensing,* 7, 11933-11953. https://doi.org/10.3390/rs70911933

Holman, F. H., Riche, A. B., Michalski, A., Castle, M., Wooster, M. J., & Hawkesford, M. J. (2016). High throughput field phenotyping of wheat plant height and growth rate in field plot trials using UAV based remote sensing. *Remote Sensing,* 8, 1031. https://doi.org/10.3390/rs8121031

James, M. R., Robson, S., d'Oleire-Oltmanns, S., & Niethammer, U. (2017). Optimising UAV topographic surveys processed with structure-from-motion: ground control quality, quantity and bundle adjustment. *Geomorphology,* 280, 51-66. https://doi.org/10.1016/j.geomorph.2016.11.021

Liu, Y., Han, K., & Rasdorf, W. (2022). Assessment and prediction of impact of flight configuration

factors on UAS-based photogrammetric survey accuracy. *Remote Sensing,* 14, 4119. https://doi.org/10.3390/rs14164119

Malambo, L., Popescu, S. C., Murray, S. C., Putman, E., Pugh, N. A., Horne, D. W., Richardson, G., Sheridan, R., Rooney, W. L. Avant, R., Vidrinec, M., McCutchen, B., Baltensperger, D., & Bishop, M. (2018). Multitemporal field-based plant height estimation using 3D point clouds generated from small unmanned aerial systems high-resolution imagery. *International Journal of Applied Earth Observation and Geoinformation,* 64, 31–42. https://doi.org/10.1016/j.jag.2017.08.014

Martínez-Carricondo, P., Agüera-Vega, F., Carvajal-Ramírez, F., Mesas-Carrascosa, F. J., García-Ferrer, A., & Pérez-Porras, F. J. (2018). Assessment of UAV-photogrammetric mapping accuracy based on variation of ground control points. *International Journal of Applied Earth Observation and Geoinformation,* 72, 1–10. https://doi.org/10.1016/j.jag.2018.05.015

Oniga, V.-E., Breaban, A.-I., Pfeifer, N., & Chirila, C. (2020). Determining the suitable number of ground control points for UAS images georeferencing by varying number and spatial distribution. *Remote Sensing,* 12, 876. https://doi.org/10.3390/rs12050876

Rangel, J. M. G., Gonçalves, G. R., & Pérez, J. A. (2018). The impact of number and spatial distribution of GCPs on the positional accuracy of geospatial products derived from low-cost UASs. *International Journal of Remote Sensing,* 39(21), 7154–7171. https://doi.org/10.1080/01431161.2018.1515508

Sanz-Ablanedo, E., Chandler, J. H., Rodríguez-Pérez, J. R., & Ordóñez, C. (2018). Accuracy of unmanned aerial vehicle (UAV) and SfM photogrammetry survey as a function of the number and location of ground control points used. *Remote Sensing,* 10, 1606. https://doi.org/10.3390/rs10101606

Ulvi, A. (2021). The effect of the distribution and numbers of ground control points on the precision of producing orthophoto maps with an unmanned aerial vehicle. *Journal of Asian Architecture and Building Engineering,* 20(6), 806-817. https://doi.org/10.1080/13467581.2021.1973479

Westoby, M. J., Brasington, J., Glasser, N. F., Hambrey, M. J., & Reynolds, J. M. (2012). “Structure-from-Motion” photogrammetry: A low-cost, effective tool for geoscience applications. *Geomorphology,* 179, 300–314. https://doi.org/10.1016/j.geomorph.2012.08.021

Xie, T., Li, J., Yang, C., Jiang, Z., Chen, Y., Guo, L., & Zhang, J. (2021). Crop height estimation based on UAV images: Methods, errors, and strategies. *Computers and Electronics in Agriculture,* 185, 106155. https://doi.org/10.1016/j.compag.2021.106155